Article

Multimode Ytterbium–Aluminosilicate Core Optical Fibre for Amplification and Laser Applications

Dunia Blaser [1,2,*], Pascal Hänzi [2], Sönke Pilz [1], Alexander Heidt [2] and Valerio Romano [1,2]

1   Institute for Applied Laser, Photonics and Surface Technologies (ALPS), Bern University of Applied Sciences, ALPS, Pestalozzistrasse 20, CH-3400 Burgdorf, Switzerland; soenke.pilz@bfh.ch (S.P.); valerio.romano@bfh.ch (V.R.)
2   Institute of Applied Physics (IAP), University of Bern, Sidlerstrasse 5, CH-3012 Bern, Switzerland; pascal.haenzi@unibe.ch (P.H.); alexander.heidt@unibe.ch (A.H.)
*   Correspondence: dunia.blaser@bfh.ch

Abstract: Rare-earth-doped optical fibres are widely used in lasers and amplifiers. The incorporation of ytterbium and aluminium oxide in a high doping concentration has led to the fabrication of a multi-mode (MM) optical fibre. Within this research, the design, preparation and calculation for the production of a fibre with a targeted 45 μm core diameter are explored. By Energy Dispersive X-ray (EDX) analysis, the doping concentrations of the elements in the core have been measured as 60.4 at.% Al and 1 at.% Yb. Supporting micrographs are used for confirming the core/cladding ratio. Based on the atomic percentage concentration, the calculated refractive index of the multi-element core has an n = 1.61 and an NA = 0.678. Characterisation of the fibre, including absorption and emission cross-section analysis, was performed in order to prove the ability of the fibre to be used for amplification as well as lasing applications.

Keywords: ytterbium fibres; alumina fibres; rare-earth optical fibres; multimode fibre; lasing applications; fibre laser; amplifier fibre

1. Introduction

Rare-earth elements have provided enormous improvements in the development of fibre lasers and amplifiers due to the unique optical properties achieved by their active 3+ ions. When incorporated into the silica glass matrix of a fibre core as co-dopants, rare-earth ions provide efficient signal amplification under excitation with an external pump light source. The design of active fibres requires careful control of the co-doping materials and the core composition. In particular, high doping concentrations of active ions and large core diameters are advantageous for scaling the repetition rate and peak power of pulsed fibre lasers and amplifiers by providing large effective areas, enabling short device lengths and increasing the threshold for the onset of detrimental nonlinear effects [1–3].

It is well known that the glass host composition is an important factor determining the solubility of rare-earth dopants in the glass matrix. Pure silica offers only poor solubility, leading to clustering and quenching effects that negatively affect fluorescence lifetime, emission and efficiency of the active fibre. In order to increase the achievable doping levels, aluminium (Al) oxide or alumina, as a passive element, is thought to play a crucial role as a network modifier by improving the solubility of the rare-earth ions and mitigating the undesirable consequences of ion clustering [4]. Hence, the main motivation for the research presented in this paper is the fabrication of an active aluminosilicate fibre containing a large percentage of alumina in the core glass matrix, with the ultimate goal of pushing the limits of achievable rare-earth ion doping concentrations, with particular focus on ytterbium (Yb).

Fabrication methods often used for the realisation of doped fibre preforms are Modified Chemical Vapor Deposition (MCVD) [3,5–8], Plasma-enhanced chemical vapor deposition (PCVD) and Inside vapor phase epitaxy (IMCVD). However, these have shown limitations

in terms of achievable geometry, doping concentration and refractive index homogeneity [5]. In contrast, sol-gel [9,10], powder-based [4,11] and Reactive Powder Sintering of Silica (REPUSIL) technologies [12] offer improved flexibility in concentration, the production of large core diameters and the ability to tailor the index step between different fibre regions.

Previous studies performed on Yb-doped optical fibres that have presented high concentrations of Al and produced with the MCVD process have shown concentrations of 1.5 to 1.7 mol% Al_2O_3 and 0.18 to 0.20 mol% Yb_2O_3, respectively [13]. Also, with the MCVD process, experiments with varying concentrations of both Al and Yb [7] have been carried out, together with a complete refractive index study based on the concentration distribution on the preform. Outstanding work with Al and possibly the highest amount of Yb found in an optical fibre by MCVD presented 1.7 mol% Yb_2O_3 and 3 mol% Al_2O_3 [1].

Studies focused on preform fabrication techniques, in which oxide powders are annealed and sintered into rods, have yielded maximum concentrations of 0.128 mol% Yb_2O_3 and 1.112 mol% Al_2O_3 [14]. Optical fibres produced with powder-based technology [10], aiming to investigate the influence of the materials on their refractive index and transmission, presented two optical fibres with ytterbium as a constant element and fixed alumina concentrations (with respect to phosphorus): Fibre 1 with 9 at.% Al and 11 at.% P and Fibre 2 with 4.5 at.% Al and 5.5 at.% P, with a constant concentration of 0.3 at.% Yb.

The optical fibre presented within this work aims to test the limits of the powder-in-tube method, which is the one implemented in order to produce it. Such limits include high doping concentrations for the powder of the core and flexibility in achieving a multi-mode (MM) optical fibre with large fibre diameters. Signal amplification and fibre lasers are some of the applications where both single-mode (SM) fibres [12–15] and large-mode area fibres (LMA) [16] can be implemented. Multi-mode fibres can transmit higher power levels (such as the ones implemented in machining or cutting), are less sensitive to misalignment and can be used over short distances.

The preform assembly implemented for the realisation of the optical fibre here presented consisted of Yb/Al-doped powder poured into a silica capillary for the core region, and the remaining gap (between the silica capillary and outer silica tube) has been filled with commercial silica (Silitec) powder for the cladding. By placing a silica capillary, a centred location and continuity of the core (waveguide) can be achieved. It has been found that an initial core powder can hardly be concentrically contained using the powder-in-powder technique; this is mainly due to the different particle sizes of the core and cladding (loose) powder. Improved methods have been developed in order to achieve better results and a stable fibre structure [17].

Within this work, results are presented on the powder-in-tube fabrication of a highly Yb/Al-doped, large core optical fibre with initial preform core doping concentrations of 3 at.% Yb and 97 at.% Al and a targeted core diameter of 45 μm. The initial powder mixture has been analysed with energy diffractive X-ray (EDX), where results showed concentrations of 2.5 at.% Yb and 97.5 at.% Al, which is close to the calculated percentage of the powder mixture. The concentrations found by EDX within the (final) optical fibre structure here presented are 60 at.% Al, 1 at.% Yb and 39 at.% Si or 43.165 mol% Al_2O_3, 0.719 mol% Yb_2O_3 and 56.116 mol% SiO_2. These concentrations have been converted as described in [18].

The effects of material diffusion between the Yb/Al core matrix and the silica cladding tube during thermal processing are discussed in detail using EDX analysis and refractive index measurements. The performance of the fabricated fibre in laser and amplifier setups is evaluated.

2. Materials and Methods

2.1. Preform and Fibre Fabrication

For the fabrication of the fibre presented in this study, the powder-in-tube technology has been used. The preform assembly consists of a thin-walled silica capillary (Ø 4/2.75 mm outer/inner diameter) that contains the Yb/Al powder prepared from a

slurry. The powder mixture consists of dissolving (separately) each precursor in ethanol, then mixing them together whilst in liquid state. The doped solution is then dried into powder by applying heat in order to evaporate the liquids, and finally, there is a post-processing powder step that includes milling and particle size selection.

The capillary is then sleeved into a larger diameter silica tube (Ø 20/17 mm), where the remaining gap is filled with pure silica powder (Silitec). Drawing was carried out at 2035 °C due to the high melting point of the core materials. Note that the drawing temperature is slightly higher than the one used for fibres with elevated amounts of alumina in the core. A weak vacuum pressure was applied in order to release gases trapped between the powder particles and control the volume shrinkage during vitrification.

The fibre was designed for a target core diameter of 45 ± 2 μm, which required a size reduction of five orders of magnitude and resulted in an outer cladding of Ø 350 μm. The un-densified preform radius of 0.01 m corresponds to a densified preform radius of 0.00885 m. This yielded a fibre drawing speed of $v_{fib} = v_{pf} \times r_{pf}^2 / r_{fib}^2 = 4.1$ m/min at 2035 °C temperature.

2.2. Characterisation Methods

The fibre produced was analysed to further understand its properties and the possibility of using it in the construction of a fibre laser and an amplifier. Due to the nature of the analysis performed, different fibre samples were used, which may result in slight variations in dimensions.

Micrographs of the fibre confirm the general structure as well as the dimensions. EDX analysis helps to understand the material behaviour in terms of diffusion effects, as silica from the cladding is expected to diffuse into the core matrix.

A qualitative 2D index mapping along with EDX results are used to estimate the refractive index profile of the fibre. Fluorescence, spectroscopy, signal gain measurements and laser operation tests demonstrate the feasibility of constructing a multi-mode fibre amplifier or fibre laser [19].

3. Results

3.1. Micrograph

The microscope image in Figure 1, taken with a 10× magnification objective, shows a cleaved and polished sample of the fabricated fibre. Core and cladding regions are well distinguishable. The sample is back-illuminated with a visible light source, and the micrograph clearly shows the guiding and transmission of the light in the core region. After calibration of the microscope with commercial fibre, the core diameter of the fabricated fibre sample was determined to be 43 μm with a cladding diameter of 350 μm. Hence, the fabricated fibre dimensions correspond well to the design target parameters.
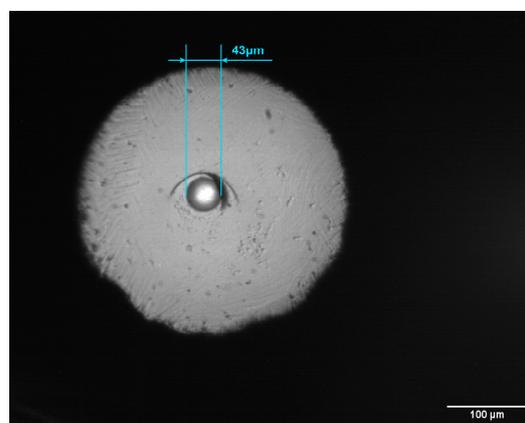
Figure 1. Micrograph of a cleaved and polished sample of the fabricated fibre. The core doped with Yb/Al shows a diameter of 43 μm, as well as transmission of visible light.

3.2. Energy Dispersive X-ray Analysis

Fibre samples have been subjected to Energy Dispersive X-ray (EDX) analysis, targeting specifically the fibre core and the central regions of the cladding immediately adjacent to the core. For a better understanding of the distributions of the elements within the fibre structure, Figure 2a shows the region chosen for a line scan performed in order to further investigate the diffusion effects associated with each element. The corresponding results of position-dependent element concentrations are plotted in Figure 2b. At the centre of the fibre core, we measure a composition of 60 at.% Al, 1 at.% Yb and 39 at.% Si. Towards the edges of the core region, the Si concentration increases and the Al concentration decreases until they reach 100% and 0%, respectively, in the cladding. Therefore, compared to the initial core composition of 97% at.% Al and 3 at.% Yb, significant diffusion effects have taken place during the fibre draw. In accordance with previous studies [17], Si is the most mobile element, and significant amounts have diffused from the Si cladding tube into the initially pure ytterbium aluminium oxide core area, while the diffusion of core material into the cladding is minimal.
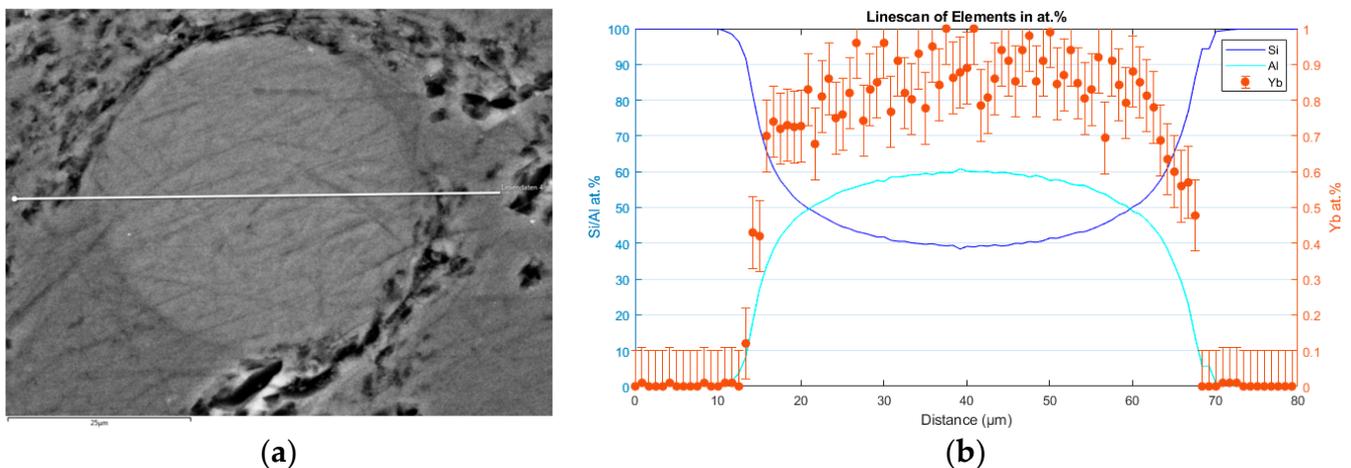
Figure 2. EDX (**a**) line scanning of elements, (**b**) graph of doping concentrations from the line scan.

Figure 2b shows the line depicting the Yb concentration in atomic percentage that was performed with a distance between point to point of 0.33 μm. Discrepancies between reading points might be caused by noise on the measurement due to being close to the limit of detection for Yb on this specific setup, which is circa 0.4 wt.%.

The initial concentration of the powder for the core was approximately 3 at.% ytterbium and 97 at.% alumina. From the EDX results performed on the final fibre samples, it can be observed that only a third of the initial concentration of Yb and about two-thirds of Al are found in the core. The diffusion phenomenon that takes place during fibre drawing, along with the different viscosity constants between Al [20], Yb and Si, are the cause for the decreasing concentrations. Therefore, for future fibre calculation and production of powder, it is highly suggested to increase the initial doping percentage of the elements. As an initial step, at least double the amount of the targeted final concentration. In other words, for a fibre sample with 3 at.% Yb in the core, aim to produce a 6 at.% Yb in the initial powder mixture. By using this calculating procedure, the decreasing doping concentrations due to diffusion effects can be further studied.

3.3. Refractive Index

In order to define the refractive index of the fibre, we implemented two different methods: (i) qualitative imaging processing using a two-dimensional refractive index (2D-RI) mapping developed within our group [21] and (ii) a theoretical calculation approach. For the theoretical approach, the percentage of the atomic concentration of each element within the core, as determined by EDX analysis, is multiplied by its specific refractive index

value (at the same wavelength) and summed up, providing a calculated index of refraction of the multi-element fibre core.

Figure 3a depicts the index map of the fibre extracted from the 2D-RI setup, which is based on a modified refractive near-field technique explained in detail in [21]. The fibre is placed into immersion oil and back-illuminated with a homogenous light source. Gray scales from an acquired microscope image can then be translated to a 2D refractive index map, using as references the known refractive indices of the oil and silica cladding with n_{oil} = 1.516 and n_{Si} = 1.46 at 633 nm, respectively. Certain areas of the fibre cladding appear to be darker compared to the rest. This is due to the hand polishing of the sample producing an uneven fibre facet, leading to a non-uniform light distribution and a slight slope in the extracted refractive index of the cladding region. The core region appears to be the brighter area, confirming that its index is higher than the ones of the cladding and immersion oil. Figure 3b shows the RI line profile obtained from the transversal line of the index map image. A noticeable delta n between cladding and core region is observed where the qualitative n of the core can be defined as ~1.51.

(a)　　　　　　　　　　　　　　　　　　　　　　**(b)**
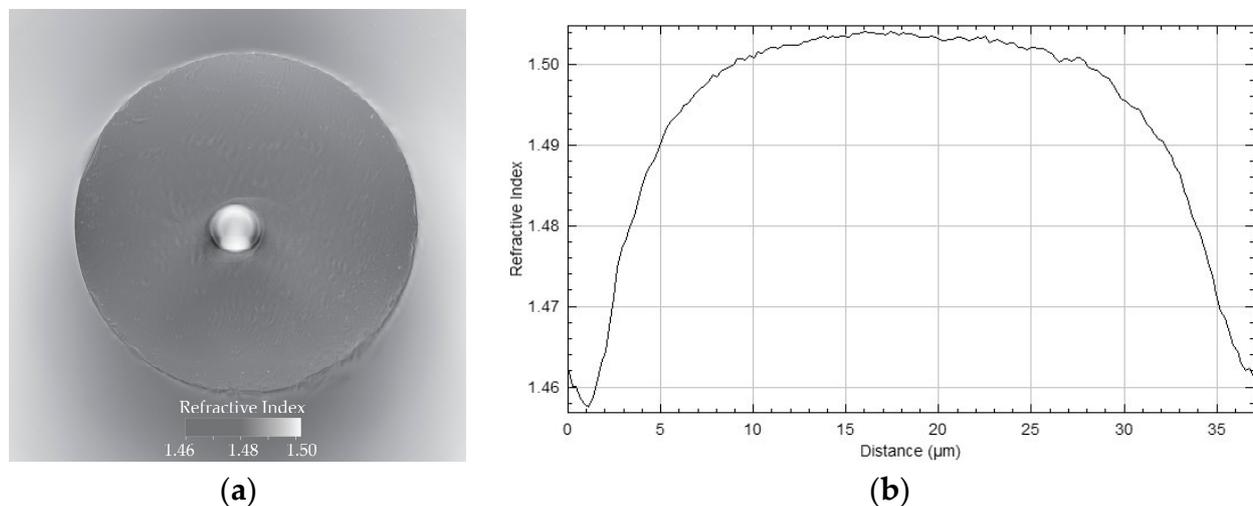
Figure 3. Qualitative 2D refractive index imaging with (**a**) index map of the fibre sample surrounded by immersion oil and (**b**) distribution of refractive index focused on the core of the fibre.

This measurement clearly shows the strong correlation between the core element composition measured by EDX and the refractive index profile of the fibre. Since Si has a significantly lower refractive index than Al and Yb (n_{Al} = 1.7 [22], n_{Yb} = 1.94 [23], n_{Si} = 1.46 [24] at 633 nm), the diffusion of Si from the cladding into the initially pure Al/Yb core matrix lowers the numerical aperture of the fibre and leads to the formation of a gradient index profile.

Due to the strong link between refractive index and core composition, we proceed to estimate the refractive index profile of the fibre by multiplying the refractive index of each element by its atomic percentage concentration, as extracted from the EDX measurements in Section 3.2. Using the previously mentioned index values for the three elements of the fibre yields a maximum refractive index at the core centre of n_{core} = 1.61, and the calculated refractive index line profile is shown in Figure 4. The discrepancy in the indices obtained from the two methods is attributed to the limited range of the 2D-RI setup. It is applicable to index differences in the range of 6×10^{-4} [21]. By having a greater index step between the silica cladding and the ytterbium–aluminosilicate core, the 2D-RI method can only provide qualitative results.
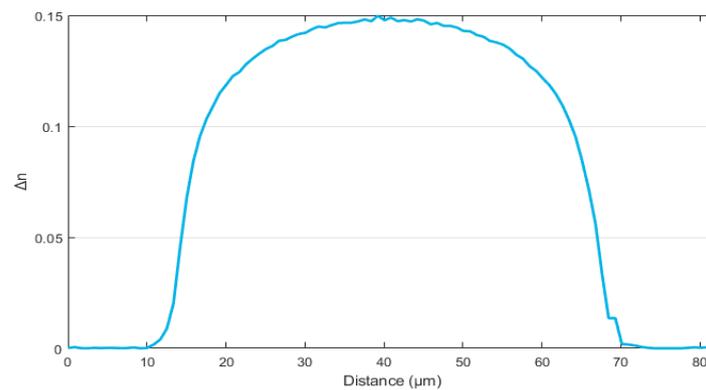
Figure 4. Calculated refractive index difference (Δn) between the multi-element doped core with respect to the silica cladding.

Based on the index of refraction obtained from the calculation method, the numerical aperture of the fibre can be defined as NA = 0.678. This is significantly higher than the NA values achieved in previous studies in fibres with lower Yb/Al concentrations [12–14].

3.4. Fluorescence and Spectroscopy

An important characteristic of rare-earth-doped optical fibres is their fluorescence lifetime, as short lifetimes are an indication of quenching effects associated with a strong non-saturable loss [25]. This is particularly relevant in highly doped fibres, such as those investigated in this study. The fluorescence lifetime of the fabricated fibre was measured at 1.2 ms, which suggests that there are no significant ion clustering and quenching effects occurring in the fabricated fibre. The measured lifetime is also significantly higher than the values in previous studies using comparable powder-based techniques with lower or similar Yb concentrations that exhibit lifetimes in the order of 0.86 ms [10].

Next, the absorption and fluorescence characteristics of the fibre were analysed. The absorption spectrum was recorded using a white-light source, and the fluorescence spectrum under 976 nm pumping was measured from the side of a short fibre sample by placing the fibre in an integrating sphere and connecting it to a spectrum analyser. By using the Füchtbauer–Ladenburg relationship and the measured fluorescence lifetime of 1.2 ms, the emission cross-section for the sample was calculated [26]. The peak of the emission cross-section was assumed to be equal to the maximum of the absorption cross-section. The results match the typical cross-section for the ytterbium-doped fibres in amplifiers [25], as shown in Figure 5.
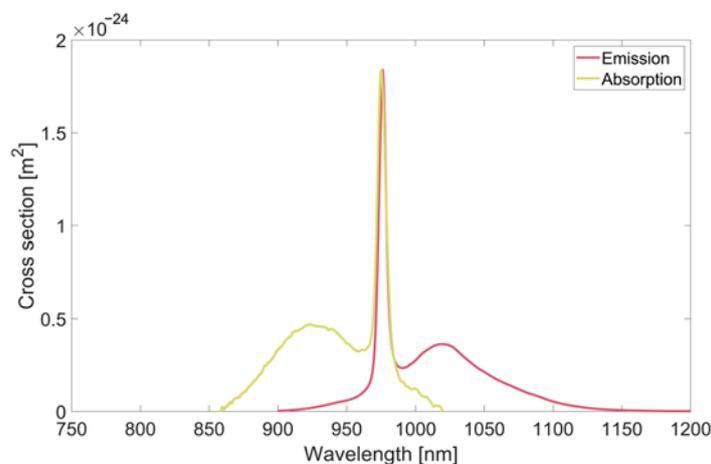
Figure 5. Measured absorption and emission cross-sections of the fabricated fibre.

3.5. Signal Amplification and Laser Operation

A fibre sample of 86 cm with low index coating was cladding-pumped at 976 nm and seeded at 1060 nm. The coupling was performed using a free-space setup, and the wavelengths were combined with a dichroic mirror (DMSP1000, Thorlabs GmbH85232 Bergkirchen, Germany). Figure 6 depicts the signal spectrum after the fibre from the seed alone, the amplified signal, as well as laser lines around 1040 nm and 1047 nm, which could be achieved without seeding the fibre and using only the cavity formed by the Fresnel reflection at the fibre ends.
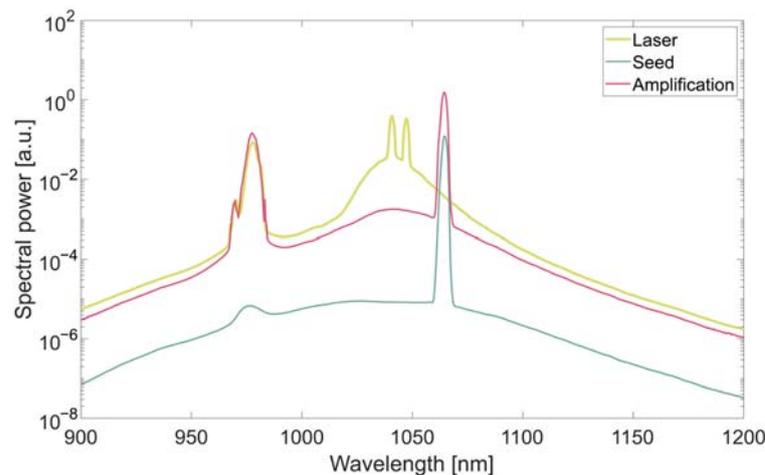
Figure 6. Spectral power of coupled laser, seed and amplified signal.

The initial seed and pump powers were set to 740 mW and 17.39 W, respectively, resulting in 2.644 W of output power and a gain of 5.53 dB (on/off 11.57 dB). For weaker seed power, the gain around 1060 nm increased to 15 dB, although a significant ASE background was observed. Note that the length of the fibre was not optimised in these experiments, and a substantial amount of pump power remained unabsorbed at the fibre end. Nevertheless, the experiments demonstrate the suitability of the fabricated fibre for lasing and amplification applications.

An additional cut-back measurement was performed with an SM fibre coupled laser at 1550 nm (Thorlabs FPL1009S), butt-coupling the light into the test fibre and output power measured with a Gentec XLP12-3S-H2-D0 powermeter. In order to perform the cut-back measurement, the initial fibre length of 4924 mm was chosen as it was the longest length that allowed for a signal to be measured by the powermeter at the other fibre end. The test fibre was cut five times, approximately 1 m in length, and cleaved at least three times for each length, aiming to ensure a good fibre end surface. The power was recorded each time, and the absorption coefficient was obtained by fitting an exponential function to the data, according to the Beer–Lambert law. This measurement gave a background loss of 1.66 dB/m. Accessibility to the data created, and further details are provided in the Data Availability Statement at the end of this manuscript.

4. Discussion and Conclusions

An optical fibre produced with the powder-in-tube technique and initial preformed core composition of 97 at.% Al and 3 at.% Yb was characterised in detail. The main motivation of the study was to investigate the limits of the powder-in-tube technique in the fabrication of active optical fibres with very large cores and a high percentage of aluminium in the core glass matrix, with the ultimate goal of increasing the achievable rare-earth ion doping concentrations while avoiding detrimental ion clustering and quenching effects.

One effect that is not often discussed in studies is the diffusion of the materials, especially when thermal processes are involved. Diffusion constants [27] of aluminium and phosphorus by MCVD deposition have been analysed previously, as well as the effect on the refractive index of the material, based on the dopant concentration of the

materials [28]. Fibre samples produced for the current research have shown diffusion of the initial elements, where silica from cladding diffuses into the Yb/Al core. When the silica and ytterbium/alumina molecules are in a molten state, they are able to move more freely. The high temperature of the drawing tower and the tension applied to the preform as the fibre is drawn cause silica molecules to diffuse into the Yb/Al matrix by concentration gradients. From the EDX results, it has been observed that silica ions migrate from high-concentration regions (cladding) to low-concentration regions (core). The silica concentration decreases as it diffuses further into the Yb/Al core, providing an ytterbium–aluminosilicate core with suitable optical properties that allow the transmission of visible light.

From EDX analysis of the drawn fibre, we found that diffusion during thermal processing and fibre drawing substantially alters the original core composition. In particular, Si is found to be the most mobile element diffusing from the cladding tube into the entire core volume. In the centre of the 45 μm diameter fibre core, we measured a composition of 60 at.% Al, 1 at.% Yb and 39 at.% Si, with the Si percentage increasing towards the edges of the core region. As the refractive index of the glass matrix decreases with increasing Si percentage, the observed diffusion effects reshape the refractive index profile from the initial step-index preform to a gradient index fibre with NA = 0.678. It is also observed that the fibre core contains only one-third of the initial preform Yb concentration, which should be taken into account in the powder preparation step.

Alternatively, studies where core composition consists of 1.112 mol.% and 2.268 mol.% Al_2O_3; and 0.128 mol.% and 0.256 mol.% Yb_2O_3, present an index difference of 0.0034 and 0.0072, respectively, and compared to the one of undoped silica glass [14]. In contrast [12], with a core composition of 4 mol.% Al_2O_3, 0.025 mol.% Ce_2O_3 and 0.025 mol.% Yb_2O_3, provided ~Δn of 0.011. Studies with elevated concentrations of alumina in the cladding region have shown index differences (compared to that of silica) of 0.02 and 0.04 [17] with concentrations of 17.5 at.% Al (9.589 mol%) and 35 at.% Al (21.212 mol%), respectively. The fibre presented here, with converted concentrations to molar percentages of 43.165 mol% Al_2O_3, 0.719 mol% Yb_2O_3 and 56.116 mol% SiO_2, exhibited a calculated core index of n = 1.61.

The long fluorescence lifetime of the fibre of 1.2 ms confirms that the high Al core glass concentration successfully suppresses ion clustering and quenching effects that were previously observed in fibres fabricated with similar techniques and comparable Yb-doping levels but lower Al concentrations. Emission and absorption cross-sections on a level with commercially available aluminosilicate fibres further underline the excellent quality of the produced fibre. Implemented in basic low-power laser and amplifier setups, the fibre showed a satisfactory performance level. However, given the large core and high doping concentrations, the true performance of the fibre should be evaluated in high-power, short-length pulsed fibre laser and amplifier configurations, which will be the subject of future research.

Conflicts of Interest: The authors declare no conflict of interest.

References

1. Bobkov, K.K.; Mikhailov, E.K.; Zaushitsyna, T.S.; Rybaltovsky, A.A.; Aleshkina, S.S.; Melkumov, M.; Bubnov, M.M.; Lipatov, D.S.; Yashkov, M.V.; Abramov, A.N.; et al. Properties of Silica Based Optical Fibres Doped with an Ultra-High Ytterbium Concentration. *J. Light. Technol.* **2022**, *40*, 6230–6239. [CrossRef]
2. Kenyon, A.J. Recent developments in rare-earth doped materials for optoelectronics. *Prog. Quantum Electron.* **2002**, *26*, 225–284. [CrossRef]
3. Podrazky, O.; Kasik, I.; Pospisilova, M.; Matejec, V. Use of alumina nanoparticles for preparation of erbium-doped fibres. In Proceedings of the IEEE Lasers and Electro-Optics Society Annual Meeting Conference Proceedings, Lake Buena Vista, FL, USA, 21–25 October 2007; pp. 246–247.
4. Renner-Erny, R.; Di Labio, L.; Lüthy, W. A novel technique for active fibre production. *Opt. Mater.* **2007**, *29*, 919–922. [CrossRef]
5. Dhar, A.; Paul, M.C.; Pal, M.; Mondal, A.K.; Sen, S.; Maiti, H.S.; Sen, R. Characterization of porous core layer for controlling rare earth incorporation in optical fibre. *Opt. Express* **2006**, *14*, 9006–9015. [CrossRef] [PubMed]
6. Webb, A.S.; Boyland, A.J.; Standish, R.J.; Yoo, S.; Sahu, J.K.; Payne, D.N. MCVD in-situ solution doping process for the fabrication of complex design large core rare-earth doped fibres. *J. Non-Cryst. Solids* **2010**, *356*, 848–851. [CrossRef]
7. Lindner, F.; Aichele, C.; Schwuchwo, A.; Leich, M.; Scheffel, A.; Unger, S. Optical properties of Yb-doped fibres prepared by gas phase doping. In Proceedings of the SPIE 8982, Optical Components and Materials XI, San Francisco, CA, USA, 1–6 February 2014. 89820R.
8. Honzatko, P.; Dhar, A.; Kasik, I.; Podrazky, O.; Matejec, V.; Peterka, P.; Blanc, W.; Dussardier, B. Preparation and characterization of highly thulium- and alumina-doped optical fibres for single-frequency fibre lasers. In Proceedings of the SPIE 8306, Photonics, Devices, and Systems V, Prague, Czech Republic, 24–26 August 2011; p. 830608.
9. Pilz, S.; Najafi, H.; Ryser, M.; Romano, V. Granulated Silica Method for the Fibre Preform Production. *Fibres* **2017**, *5*, 24. [CrossRef]
10. El Sayed, A.; Pilz, S.; Najafi, H.; Alexander, D.T.L.; Hochstrasser, M.; Romano, V. Fabrication and Characteristics of Yb-Doped Silica Fibres Produced by the Sol-Gel Based Granulated Silica Method. *Fibres* **2018**, *6*, 82. [CrossRef]
11. Leich, M.; Just, F.; Langner, A.; Such, M.; Schötz, G.; Eschrich, T.; Grimm, S. Highly efficient Yb-doped silica fibres prepared by powder sinter technology. *Opt. Lett.* **2011**, *36*, 1557–1559. [CrossRef] [PubMed]
12. Leich, M.; Jäger, M.; Grimm, S.; Hoh, D.; Jetschke, S.; Becker, M.; Bartelt, A.H.H. Tapered large-core 976 nm Yb-doped fibre laser with 10 W output power. *Laser Phys. Lett.* **2014**, *11*, 045102. [CrossRef]
13. Unger, S.; Lindner, F.; Aichele, C.; Leich, M.; Schwuchow, A.; Kobelke, J.; Dellith, J.; Schuster, K.; Bartelt, H. A highly efficient Yb-doped silica laser fibre prepared by gas phase doping technology. *Laser Phys.* **2014**, *24*, 035103. [CrossRef]
14. Velmiskin, V.V.; Egorova, O.N.; Mishkin, V.; Nishchev, K.N.; Semjonov, S. Active material for fibre core made by powder-in-tube method: Subsequent homogenization by means of stack-and-draw technique. In Proceedings of the SPIE 8426, Microstructured and Specialty Optical Fibres, Brussels, Belgium, 16–19 April 2012; p. 84260I.
15. Ye, C.; Petit, L.; Koponen, J.; Hu, I.-N.; Galvanauskas, A. Short-Term and Long-Term Stability in Ytterbium-Doped High-Power Fibre Lasers and Amplifiers. *IEEE—Sel. Top. Quantum Electron.* **2014**, *20*, 188–199.
16. He, W.; Leich, M.; Grimm, S.; Kobelk, J.; Zhu, Y.; Bartelt, H.; Jäger, M. Very large mode area ytterbium fibre amplifier with aluminum-doped pump cladding made by powder sinter technology. *Laser Phys. Lett.* **2015**, *12*, 015103. [CrossRef]
17. Blaser, D.; Pilz, S.; Pedrido, C.; Romano, V. High alumina content optical fibres by powder methods. In Proceedings of the SPIE 12140, Micro-Structured and Specialty Optical Fibres VII, Strasbourg, France, 3 April–23 May 2022; p. 1214008.
18. Romano, V.; Pilz, S.; Najafi, H. Powder Process for fabrication of Rare Earth-Doped Fibers for Lasers and Amplifiers. In *Handbook of Optical Fibers (S. 1-43)*; Springer Nature: Singapore, 2018. [CrossRef]
19. Devautour, M.; Roy, P.; Février, S.; Pedrido, C.; Sandoz, F.; Romano, V. Nonchemical-vapor-deposition process for fabrication of highly efficient Yb-doped large core fibres. *Appl. Opt.* **2009**, *48*, G139–G142. [CrossRef] [PubMed]
20. Blomquist, R.A.; Fink, J.K.; Leibowitz, L. *Viscosity of Molten Alumina*; Argonne National Laboratory: Lemont, IL, USA, 1978.
21. El Sayed, A.; Pilz, S.; Ryser, M.; Romano, V. Two-dimensional refractive index profiling of optical fibres by modified refractive near-field technique. In Proceedings of the SPIE 9744, Optical Components and Materials XIII, San Francisco, CA, USA, 13–18 February 2016; p. 97440N.
22. Filmetrics. Available online: https://www.filmetrics.com/refractive-index-database/Al2O3 (accessed on 8 June 2023).
23. Medenbach, O.; Dettmar, D.; Shannon, R.D.; Fischer, R.X.; Yen, W.M. Refractive index and optical dispersion of rare earth oxides using a small-prism technique. *J. Opt. A Pure Appl. Opt.* **2001**, *3*, 174. [CrossRef]
24. Malitson, I.H. Interspecimen Comparison of the Refractive Index of Fused Silica. *J. Opt. Soc. Am.* **1965**, *55*, 1205–1208. [CrossRef]
25. Paschotta, R.; Nilsson, J.; Tropper, A.C.; Hanna, D.C. Ytterbium-doped fibre amplifiers. *IEEE J. Quantum Electron.* **1997**, *33*, 1049–1056. [CrossRef]
26. Barnes, W.L.; Laming, R.I.; Morkel, P.R.; Tarbox, E.J. Absorption-emission cross-section ratio for Er^{3+} doped fibre at 1.5 μm. In Proceedings of the Lasers and Electro-Optics Conference, Anaheim, CA, USA, 21–25 May 1990; Optica Publishing Group: Washington, DC, USA; p. JTUA3.

27.　Zimer, H.; Kozak, M.; Liem, A.; Flohrer, F.; Doerfel, F.; Riedel, P.; Linke, S.; Horley, R.; Ghiringhelli, F.; Desmoulins, S.; et al. Fibres and fibre-optic components for high-power fibre lasers. In Proceedings of the SPIE 7914, Fiber Lasers VIII: Technology, Systems, and Applications, San Francisco, CA, USA, 22–27 January 2011; p. 791414.

28.　Kirchhof, J.; Unger, S.; Schwuchow, A.; Jetschke, S.; Knappe, B. Dopant Interactions in High-Power Laser Fibres. In Proceedings of the SPIE 5723, Optical Components and Materials II, San Jose, CA, USA, 22–27 January 2005; pp. 261–272.